Electrical Power Quality and Utilisation, Journal *Vol. XIII, No. 1, 2007*

Assessment of Fault Location in Power Distribution Networks

Alberto BORGHETTI, Mauro BOSETTI, Mauro Di SILVESTRO, Carlo Alberto NUCCI, Mario PAOLONE, Lorenzo PERETTO, Elisa SCALA, Roberto TINARELLI

Università di Bologna, ITALY

***Summary*: Methods aimed at locating the position where a fault is occurred can be seen as part of a complex measurement system oriented at more general power quality purposes. This paper faces the comparison between two methods recently proposed in literature for fault-location in distribution networks, based on a distributed and on a single-ended measurement system, respectively. By assuming a common distribution system topology, the two methods are applied in order to compare their performances as well as the obtained results. On the basis of the different drawbacks and advantages shown by the two methods, potential improvements are eventually taken into account, and a possible integration of the two approaches is investigated and discussed.**

1. INTRODUCTION

Increasing research interest is dedicated to faults location estimation in distribution power systems, as well as, more comprehensively, to detect and classify transient voltages according to their origin.

The problem of locating the source of faults has been extensively tackled in the literature, see [1–10]. The methodologies that have been proposed can be grouped into three main categories: i) methods based on impedance measurement [1–3]; ii) methods based on the analysis of travelling waves [4–7]; iii) expert systems based on the application of neural networks [8–10]. As far as methods i) are concerned, they essentially rely on the measurement of the fault impedance at power frequency, carried out by processing the voltage and current signals recorded at the line terminals. Transmission lines are the typical application field of this technique: the knowledge of the lines length on the one hand, and the relatively simple network topology on the other hand, allow a good accuracy achievement. When the lines are shorter and the network has radial topology (as in distribution systems) methods ii) are usually preferred, although their implementation requires for more complex measurement and processing techniques. Methods ii) rely on the analysis of the high-frequency components of voltages and currents during the propagation of the fault-originated disturbance. In this respect, wavelet-based analysis is often employed. Finally, iii) the application of neural networks has been sometimes proposed: the required training stage can also be performed by means of a great number of simulations.

In this paper two methods proposed by the Authors for locating the source of faults are briefly reviewed and applied to the same distribution test network. Both methods can be considered belonging to category ii), even if their approaches differ significantly. The first method [11] is based on the use of a distributed measurement system: the source is located by measuring in all the nodes of the monitored network the starting instants of the transient originated by the fault. The network topology must be known. The second method [12] is based on the use of the Continuous Wavelet Transform (CWT) to detect single frequencies that characterize the voltage transients generated by the fault. These frequencies can be used to infer the fault location, given the network topology and line conductor geometry, needed to determine the modal quantities of the multi-conductor line.

The paper is organized as follows. Section 2 summarizes the main features of the two approaches above mentioned. In Section 3, the assumed test network and the relevant EMTP (Electro-Magnetic Transient Program) model are described. Finally, Section 4 compares the results and the performances achieved by using the two methods.

2. THE TWO METHODS PROPOSED FOR FAULT LOCATION

In the following, the methods based on the measurement of the transient starting instants and the method based on the use of the CWT will be referred to as method A and method B, respectively.

2.1. Method A

As mentioned in the previous Section, method A relies on a proper processing procedure of the starting instants of the voltage transient originated by the fault, measured in the monitored nodes of the network by using a distributed system. Its architecture is of master-slave type: a given number of slave units are located in all the nodes of the network. Each slave unit acquires both the starting instant and the waveform of the voltage transient. The former information is sent to the master unit, which locates the transient voltage source by relating the starting instants at all the slaves units to the stored characteristics of the network. Figure 1 shows the schematic block diagram of a slave unit: the dashed box contains the blocks performing the measurement of the transient starting instant. The voltage $u(t)$ at the monitored node is conditioned by a Voltage-to-Voltage Transducer (VVT), whose output u_{VVT} feeds an Event Detection Block

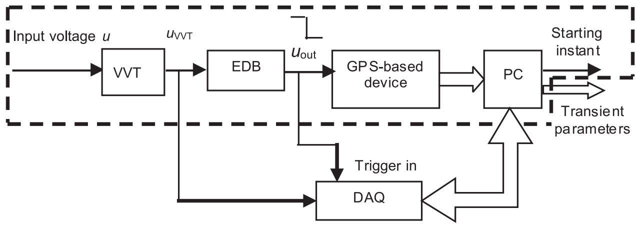

Fig. 1. Block diagram of a remote unit

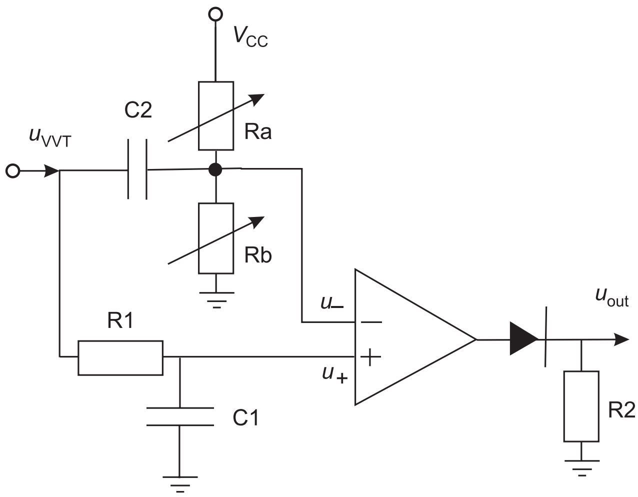

Fig. 2. Circuit implementing the event detection block (EDB)

(EDB). The EDB output u_{out} is a logic signal that, as a transient occurs, triggers both a Data AcQuisition board (DAQ) and a GPS-based device, which provides the relevant "time stamp". Figure 2 is the scheme of the operating principle implemented by the EDB [13]. First, the input signal u_{VVT} is low-pass filtered by the R_1–C_1 filter, which features a cut-off frequency of 1,600 Hz. This value allows the filter both to properly attenuate the transient affecting the transducer output and to make negligible the delay affecting the filter output u_+, due to the filter itself. Quantity u_{VVT} is also sent to the net C_2–R_a–R_b, which sums to u_{VVT} a negative bias provided by the trimmer-resistive divider R_a–R_b. Then, the operational amplifier compares the obtained signals: when $u_- > u_+$, a transient has occurred and the amplifier output must turn into the low level of a TTL signal. To this purpose, the high speed switching diode and the resistor R_2 are used to limit the low level of the comparator to 0 V. The falling edge of u_{out} is detected by a GPS-based device GPS168PCI. It provides the relevant time stamp with a resolution of 100 ns and a nominal accuracy of ± 250 ns.

Once the master unit has collected all the time stamps provided by the slave units, it applies a proper fault location procedure. To this purpose, it is assumed that: a) the network characteristics (topology, geometry, conductor spacing and type) are known; b) M slave units are installed in correspondence of each node of the network; c) the reference propagation interval between two adjacent nodes are known. Assumption a) does not appear a particular problem in practical cases. Assumption c) can also be fulfilled, for example, by carrying out proper EMTP simulations, for the various fault types.

The implemented procedure relies on the obvious concept that the larger the distance between the slave monitoring unit and the fault location, the greater the relevant time stamp value. Let us use the following notation:

t_{mk} time stamp of the starting instant of the transient voltage measured at the generic mth node ($1 \le m \le M$) on the kth phase ($k = a, b, c$ in the case of a three-phase network);

D_{nk} distance between two generic adjacent nodes, which form the nth couple ($1 \le n \le M$-1);

$T_{nk\mathrm{ref}}$, $T_{nk\mathrm{meas}}$ reference propagation time between two generic adjacent nodes and difference between the relevant measured time stamps, respectively. $T_{nk\mathrm{meas}}$ is always lower than $T_{nk\mathrm{ref}}$ when the fault is located within the line.

Due to the effects of various error sources, also for the case of a fault outside the line between the nth couple of nodes, the latter value may be different from the former one. A brief discussion on these error sources is reported in Section 4. The algorithm running on the master unit determines, for each phase and each couple of adjacent nodes, the quantity:

$$\Delta_{nk} = \frac{T_{nk_{\mathrm{ref}}} - T_{nk_{\mathrm{meas}}}}{T_{nk_{\mathrm{ref}}}} \qquad (1)$$

which ranges from zero to unity, depending on whether the fault is occurred outside or at the midst, respectively, of the considered line. Then, the algorithm seeks the maximum for Δ_{nk}, which we denote by $(\Delta_{nk})_{\max}$. Such value identifies both the faulted phase and the couple of nodes within which the fault is occurred. Finally, the distance d between the fault location and the nearest node (which is the one identified by the lower time stamp) is determined by means of the following relationship:

$$d = \frac{D_{nk}}{2}(\Delta_{nk})_{\max} \qquad (2)$$

This relationship can be explained by considering the section between two generic adjacent slaves m and m+1, separated by the distance D_{nk}. Let us assume that the transient event starts in point 0 on the considered line at time instant t=t_0 and is detected by the slaves m and m+1 at instants tmk and $tm+1k$, respectively. If Tnk_{ref} is the propagation time interval relevant to the considered section, the distances of the transient source position 0 from the slaves m and m+1 can be expressed respectively as follows:

$$d = \frac{D_{nk}}{T_{nk_{ref}}}(t_{\mathrm{mk}} - \mathrm{t}_0) \qquad (2.a)$$

$$D_{nk} - d = \frac{D_{nk}}{T_{nk_{ref}}}(t_{\mathrm{m+1\ k}} - \mathrm{t}_0) \qquad (2.b)$$

Let us remember that d is the distance between the point 0 and the closest slave. By subtracting (2.b) to (2.a) we get:

$$2d = \frac{D_{nk}}{T_{nk_{ref}}}(t_{mk} - t_{m+1k}) + D_{nk} \quad (2.c)$$

By denoting $Tnk_{\mathrm{meas}} = (t_{mk} - t_{m+1k})$ the distance d and thus equation (2) are finally determined.

2.2. Method B

Different contributions in the literature present fault location algorithm based on the analysis of travelling waves. These travelling waves can be generated by (i) current or voltage pulse generators and (ii) the fault itself. The generated travelling waves are propagating along the network and reflected in correspondence of (i) line terminations and (ii) the fault location. The relevant reflection coefficients depends to: (i) the impedances of the power components connected at the network terminations and (ii) the fault impedance.

Assuming that the generated travelling waves are measured in correspondence of a specific network node (typically on the medium voltage side of the station transformer), a certain number P of paths covered by the travelling waves can be associated to this specific measurement point. The number of paths is equal to the number of network laterals and it is possible to correlate each path to a characteristic frequency. Such frequencies can be determined a priori on the basis of the network topology and travelling wave speeds for the various propagation modes as follows:

$$f_{p,i} = \frac{v_i}{n_p L_p} \quad (3)$$

where:

- v_i is the travelling speed of the i-th propagation mode;
- L_p is the length of the p-th path;
- $n_p(\in N)$ is a coefficient indicating the number of times that the specific path is travelled in order to obtain the same polarity of the travelling wave; a more comprehensive discussion regarding the meaning of this coefficient is provided in the next sections;
- $f_{p,i}$ is the characteristic frequency associated to the p-th path and i-th mode.

The identification of these frequencies, obtained by processing the voltage or current waveforms acquired at the considered measurement point, provides P-identified frequencies. P-1 are used to identify the faulted branch of the radial network and the remaining one to identify the fault location in the faulted line [12] (see section 4). The identification of such frequencies is based on the application of the CWT on the voltage transient waveforms recorded in correspondence of the medium voltage side of the station transformer.

Let us briefly recall the main features of this transform. The CWT of a signal $s(t)$ is the integral of the product between $s(t)$ and the so-called daughter-wavelets, which are time translated and scale expanded/compressed versions of a function having finite energy $\psi(t)$, called mother wavelet. This process, equivalent to a scalar product, produces wavelet coefficients $C(a,b)$, which can be seen as "similarity indexes" between the signal and the so-called daughter wavelet located at position b (time shifting factor) and positive scale a:

$$C(a,b) = \int_{-\infty}^{\infty} s(t) \frac{1}{\sqrt{a}} \psi^*(\frac{t-b}{a}) dt \quad (4)$$

where * denotes complex conjugation.

Equation (3) can be expressed also in frequency domain [14]:

$$F(C(a,b)) = \sqrt{a}\psi^*(a \cdot \omega)S(\omega) \quad (5)$$

where $F(C(a,b))$, $S(\omega)$ and $\psi(\omega)$ are the frequency-domain representation of $C(a,b)$, $s(t)$ and y(t) respectively. Equation (4) shows that if the mother wavelet is a band-pass filter function in the frequency-domain, the use of CWT in the frequency-domain allows for the identification of the local features of the signal. According to the Fourier transform theory, if the center frequency of the mother wavelet $\psi(\omega)$ is F_0, then the one of $\psi(a\omega)$ is F_0/a. Therefore, different scales allows the extraction of different frequencies from the original signal – larger scale values corresponding to lower frequencies – given by the ratio between center frequency and bandwidth. Opposite to the windowed-Fourier analysis where the frequency resolution is constant and depends on the width of the chosen window, in the wavelet approach the width of the window varies as a function of a, thus allowing a kind of time-windowed analysis, which is dependent on the values of scale a.

Several mother wavelets have been used in the literature (e.g. [15–17]). In this paper, the so-called Morlet wavelet is chosen as mother one $\psi(t)$:

$$\psi(t) = e^{-t^2/2} e^{j2\pi F_0 t} \quad (6)$$

CWT can operate at any scale, specifically from that of the original signal up to some maximum scale. CWT is also continuous in terms of shifting: during computation, the analyzing wavelet is shifted smoothly over the full domain of the analyzed function.

The CWT analysis is performed in time domain on the voltage transients recorded after the fault in a bus of the distribution network.

The analyzed part of the transient recorded signal $s(t)$, which can correspond to a voltage or current fault-transient, has a limited duration (few milliseconds, depending on the extension of the considered network) corresponding to the product between the sampling time T_s and the number of samples N. The numerical implementation of the CWT is obtained from (4) by substituting t and b with nT_s and iT_s, respectively:

$$C(a,iT_s) = T_s \frac{1}{\sqrt{|a|}} \sum_{n=0}^{N-1} \psi^* \left[\frac{(n-i)T_s}{a} \right] s(nT_s) \quad (7)$$

where $i = 0, 1, \ldots, N$-1. The signal energy $E_{cwt}(a)$, i.e. the sum of the squared values of all coefficients corresponding to the same scale:

$$E_{cwt}(a) = \sum_{n=0}^{N-1} C^2(a, nT_s) \quad (8)$$

identifies a 'scalogram' which provides the weight of each frequency component. By inspecting the relative maximum peaks of the obtained scalogram $E_{cwt}(a)$, the most significant frequency components of the signal are detected. Let us refer to these frequency components as 'CWT-identified frequencies' of the transient. As mentioned above, the CWT-identified frequencies can be correlated to the propagation paths of the fault-originated waves, traveling along the lines, and to their reflections at discontinuity points.

Again, these theoretical frequencies can be determined a priori, provided the network topology and propagation speeds for the various fault types are known. When a fault occurs, the analysis of $E_{cwt}(a)$, obtained by processing the voltage signal acquired at the considered measurement point, provides P CWT-identified frequencies [12].

As known, the propagation of traveling waves in multiconductor transmission lines can be seen a linear combination of different propagation modes characterized by different propagation speeds [18]. The M-phase transmission line equations become simpler if the M-coupled equations are transformed to M-decoupled equations and can be solved as single-phase equations. Equations (8) and (9) show such a modal transformation, through transformation matrices $[T_e]$ and $[T_i]$ adopted for voltages and currents respectively.

$$\left[\frac{d^2V^{ph}}{dx^2}\right] = [Z'][Y'][V^{ph}]$$
$$\left[\frac{d^2I^{ph}}{dx^2}\right] = [Y'][Z'][I^{ph}] \quad (8)$$

$$[V^{ph}] = [T_e][V^m]$$
$$[I^{ph}] = [T_i][I^m] \quad (9)$$

$$\left[\frac{d^2V^m}{dx^2}\right] = [\gamma]^2[V^m]$$
$$\left[\frac{d^2I^m}{dx^2}\right] = [\gamma]^2[I^m] \quad (10)$$

where the *ph* and *m* denote phase and modal variables, Z' and Y' are the impedance and admittance matrix in per unit of length, $[\gamma]^2$ is the diagonal matrix of the common eigenvalues of products $[Z'][Y']$ and $[Y'][Z']$, being $\gamma_i = \alpha_i + j\beta_i$ the propagation constant of mode i, α_i the attenuation constant and β_i the phase constant of mode i. The phase velocity of mode i is given by:

$$v_i = \frac{\omega}{\beta_i} \quad (11)$$

Considering that multi-conductor distribution lines are usually unbalanced, the calculation of the matrixes $[T_e]$ and $[T_i]$, which must be real in order to be adopted in a time-domain application of the CWT, is performed using EMTP.

The implementation of method B does not require the use of a distributed system with a slave unit at each bus, although in complex and large distribution networks multiple measurement points would allow improved performances.

3. APPLICATION EXAMPLES

Computer simulations have been carried out to compare both the considered approaches. EMTP-RV [19,20] has been used to simulate the transient response of a faulted distribution test network, whereas MATLAB scripts were developed in order to emulate all the instrumentation and processing devices required by the two methods.

Figure 3 shows the considered distribution test network, composed by a 10-km long main feeder (lines L1, L2 and L3) and by two laterals of 2-km length (L4) and 1-km length (L5). The overhead lines are assumed balanced, therefore transformation matrixes $[T_e]$ and $[T_i]$ of equations (8) and (9) are identical and real, being the Clarke's $(0, \alpha, \beta)$ transformation matrix [18].

The power distribution network is fed through a 150/20 kV substation G, whose transformer T has a Yg/d connection.

Figure 4 illustrates the load blocks connected at bus 1, 2 and 3 of Figure 3. Each load is connected at the low voltage side of a 20/0.4 kV distribution transformer and it is represented by three impedances. Capacitances are also included in parallel at each transformer model in order to

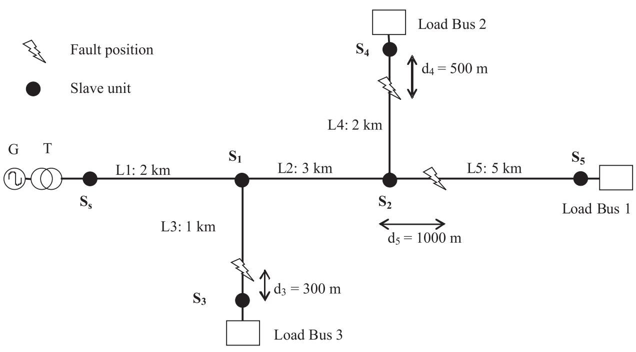

Fig. 3. The test network (not in scale)

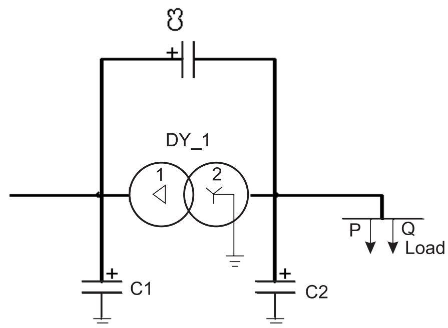

Fig. 4. Configuration of the load blocks

simulate, in a first approximation, its response to transients at a frequency range around 100 kHz.

Phase-to-ground and three-phase short circuits have been simulated at three different locations, shown by flashes in Figure 3, by using ideal switches, closed at 1.5 ms. For the sake of brevity, in the following are reported the results relevant to two of the three fault positions considered during simulations. For the application of Method A, six slave units of the distributed measurement system are supposed to be placed in all the network nodes, shown by black bullets in the figure and denoted by S_s, S_1, S_2, S_3, S_4 and S_5. For Method B, the voltage transients are assumed to be recorded by unit S_s.

For method A, the simulation time step was set to 10 ns to grant the typical time resolution of an analog device such as the EDB of Figure 2. Method B has been applied by assuming 1 μs of simulation time step in order to emulate a 1 MSa/s sampling frequency of the DAQ. The values of $T_{nk\mathrm{ref}}$, required by method A, have been obtained by the simulation of the propagation of a voltage pulse injected at bus S_s.

4. RESULTS AND DISCUSSION

The discussion is here limited to the results relevant to faults (phase-to-ground and three phase short circuits) in line L3 and L5, because it could be applied to faults located in all the other branches of the considered distribution network.

4.1. Faults in line L3

The fault location is 300 m away from the nearest node (bus S_3) and 2.7 km from S_s. Table 1 shows the values of Δ_{nk} estimated for all the node couples and for both types of fault. In both this table and the following ones, the values of $(\Delta_{nj})_{max}$ are in bold characters. Line L3, defined by the slave units located in S_1 and S_3, is correctly identified as faulted.

Table 1. Values of Δnj (p.u) in the case of fault in line L3.

Nodes couples	Phase-to-ground fault Δ_{na}	Δ_{nb} (·10⁻²)	Δ_{nc}	Three-phase fault Δ_{na}	Δ_{nb} (·10⁻²)	Δ_{nc}
S_s- S_1	0.04	0.04	0.04	0.04	0.04	0.04
S_1- S_2	0.14	0.14	0.14	0.14	0.14	0.14
S_1- S_3	**60**	**60**	**60**	**60**	**60**	**60**
S_2- S_4	0.04	-0.11	-0.11	0.04	-0.11	0.04
S_2- S_5	0.04	0.04	0.04	0.04	-0.02	0.04

The application of (2) provides values of *d* equal to 300.1 m and 300.6 m for phase-to-ground and three-phase short circuit, respectively.

As far as method B is concerned, Figure 5 illustrates six paths covered by travelling waves originated by a fault in the line L3. The travelling waves are reflected at the line terminations and at the fault location. Paths with partial reflections at the point where more lines converged are here disregarded. Only three paths (namely paths 3, 1 and 2) reach the observation point, assumed at bus S_s.

As mentioned in section 2.2, it is possible to correlate each path to characteristic frequencies of the fault transient recorded at the observation point by the following considerations: path 3 is associated to a period given by a travelling time equal to 4 times L1+0.7*L3 divided by the propagation speed of the considered propagation mode (see equation (11)), as the travelling wave experience reflections of opposite sign at the fault location and at the sending end of the main feeder. For paths 1 and 2, the associated periods are given by the travelling time relevant to the double path lengths (L1+L2+L4 and L1+L2+L5, respectively), as the travelling wave is reflected at the line terminations.

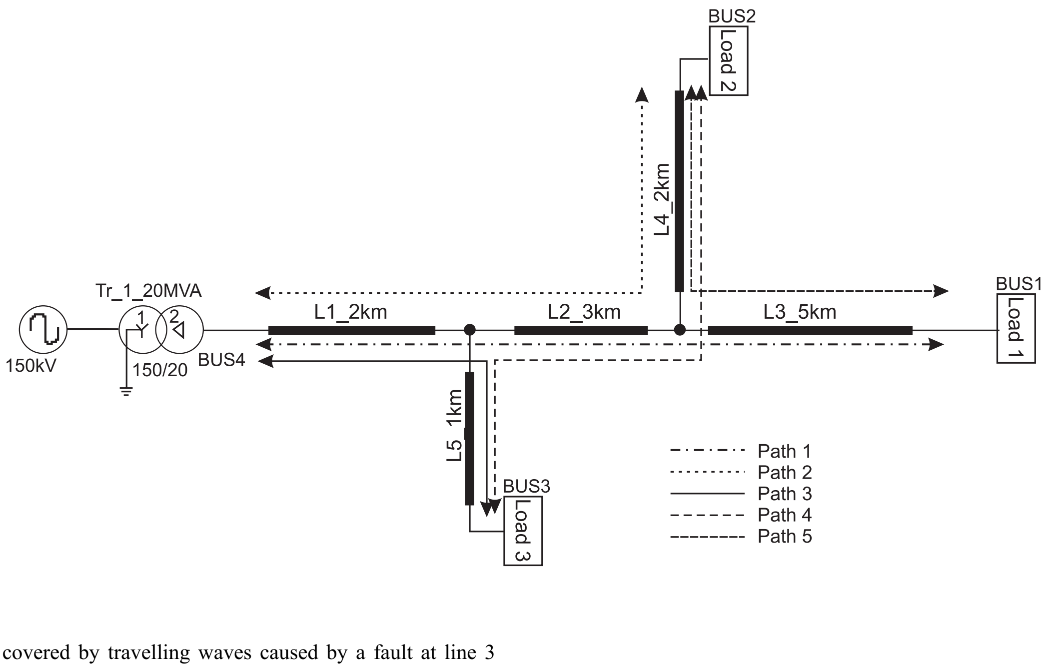

Fig. 5. Paths covered by travelling waves caused by a fault at line 3

Table 2. Frequency values theoretically associated to the paths covered by the travelling waves of mode β, originated by a balanced three-phase fault at line L3, and values identified by the CWT analysis.

Path	Length (km)	Theoretical frequency value (traveling wave at light speed) (Hz)	CWT identified frequency value (kHz)	Fault distance error from bus S_s (m)
L1+0.7•L3	4•2.7	27.2	30.0	
L1+L2+L4	2•7	21.0	19.6	249.2
L1+L2+L5	2•10	14.7	14.7	

Table 3. Frequency values theoretically associated to the paths covered by the travelling waves of mode 0 originated by a phase-to-ground fault at line L3, and values identified by the CWT analysis.

Path	Length (km)	Theoretical frequency value (traveling wave at light speed) (Hz)	CWT identified frequency value (kHz)	Fault distance error from bus S_s (m)
L1+0.7•L3	4•2.7	22.5	28.8	
L1+L2+L4	2•7	17.3	14.0	533.9
L1+L2+L5	2•10	12.1	8.8	

Table 4. Values of Δ_{nj} (p.u) in the case of fault in line L5

Nodes couples	Phase-to-ground fault			Three-phase fault		
	Δ_{na}	Δ_{nb}	Δ_{nc}	Δ_{na}	Δ_{nb}	Δ_{nc}
		$(\cdot 10^{-2})$			$(\cdot 10^{-2})$	
S_s- S_1	-0.11	-0.11	-0.11	0.04	-0.11	0.04
S_1- S_2	0.14	0.14	0.14	0.14	0.14	0.14
S_1- S_3	-0.25	-0.25	-0.25	0.04	-0.25	0.04
S_2- S_4	0.04	0.04	0.04	0.19	0.04	0.04
S_2- S_5	**40**	**40**	**40**	**40**	**40**	**40**

The results of the CWT analysis of the propagation mode β relevant to the voltage transient due to a three phase fault at line L3 observed in the node S_s produce the identified frequencies shown in Table 2 that reports also the fault distance error from bus S_s estimated by using the identified frequency relevant to the fault path L1+0.7*L3. The fault location error ΔL_p is calculated, by means of equation (3), as:

$$\Delta L_p = L_p^* - \frac{v_\beta}{n_p f_\beta}$$

where:

L_p^* is the length of the faulted path,
v_β is the propagation speed of the CWT-analyzed mode,
f_β is the CWT-identified frequency corresponding to the propagation path.

Table 3 presents the results of the CWT analysis of the propagation mode 0 relevant to the voltage transient due to a phase-to-ground fault at line L3 observed in the node S_s.

4.2. Faults in line L5

The fault location is 1000 m away from the slave unit S_2, located in the nearest node, and 5 km away from S_s. Table 4 reports the relevant values of Δ_{nk}. The line L5, defined by the slave units located in S_2 and S_5, is correctly identified as faulted. The application of (2) provides values of d equal to 1000.6 m for both phase-to-ground and three-phase short circuit.

Table 5 presents the results of the CWT analysis of propagation mode β relevant to the voltage transient due to a balanced three-phase fault at line L5 observed in the node S_s. For this case the fault location error is of 553.7 m. In the case of phase-to-ground fault, Table 6 shows that the location error is 1261.7 m.

Some considerations can be drawn from the results presented in Tables 2-6. First of all, method A correctly identifies the line where the transient occurs and computes with a good accuracy the distance between the source and the nearest node. However, values of Δ_{nj} different from zero are found also for non-faulted lines. Reasonably, this is due to the superposition of direct and reflected waves, which, case by case, modify the voltage waveforms. The impact of this error turns into a reduced sensitivity when computing distance d. Indeed, when the transient source is located close to a node, the value of the relevant Δ_{nj} could not be $(\Delta_{nj})_{\max}$; in such a case the method would not provide correct information. In the results that we have shown, the largest incorrect value of Δ_{nj} is in the order of $0.25 \cdot 10^{-2}$, which corresponds to a resolution $d_{min} = 0.125\% \cdot D_{nk}$. By considering the longest line in the network of Figure 3 (line between S_2 and S_5), it is $d_{min} \approx 6$ m. However, by considering the effect of the uncertainty associated with the time stamp provided by the GPS-based device, which turns approximately into an expanded uncertainty $U(d) = 3 \cdot u_c(d) \approx 180$ m, it results $d_{min} \ll U(d)$. It is worth mentioning that the practical implementation of such a method is somewhat expensive. As a matter of fact, the cost can be presently estimated of the order of 7,000 Euro for each unit, mainly due to the need of three wide-band voltage-to-voltage transducers and a GPS receiver. However, these costs are expected to decrease in the near future.

As far as method B is concerned, it correctly identifies the faulted line but the accuracy on the fault location is not

Table 5. Frequency values theoretically associated to the paths covered by the travelling waves of mode ß originated by a balanced three-phase fault at line L5, and values identified by the CWT analysis.

Path	Length (km)	Theoretical frequency value (traveling wave at light speed) (Hz)	CWT identified frequency value (kHz)	Fault distance error from bus S_s (m)
L1+L2+0.2•L5	4•6	12.3	13.5	
L1+L2+L4	2•7	21.0	25.5	553.7
L1+L3	2•3	49.0	48.5	

Table 6. Frequency values theoretically associated to the paths covered by the travelling waves of mode 0 originated by a phase-to-ground fault at line L5, and values identified by the CWT analysis.

Path	Length (km)	Theoretical frequency value (traveling wave at light speed) (Hz)	CWT identified frequency value (kHz)	Fault distance error from bus S_s (m)
L1+L2+0.2•L5	4•6	10.1	12.8	
L1+L2+L4	2•7	17.3	18.8	1261.7
L1+L3	2•3	40.4	37.2	

completely satisfactorily, even if the uncertainty on the identified frequency (about 2% [12], which corresponds to 150 m) is taken into account. This is due to two main reasons: a) the chosen mother wavelet; b) the use of a single-point measurement system. Indeed, it is well known that the results of a wavelet analysis are strictly related to the chosen mother wavelet; in this respect, the Morlet function probably is not the best option for this application. The use of the information provided by more than one measurement point could improve the accuracy of the method.

5. CONCLUSIONS

Two methods proposed by the Authors for fault location in power distribution networks have been reviewed and compared, by means of EMTP simulations, for the case of a typical medium voltage network configuration.

The complementary characteristics of the two considered methods suggest the analysis of an hybrid approach based on the combined use of the two types of information, i.e. starting time and wavelet analysis of voltage transients recorded at some location.

In particular, for the typical configuration of medium voltage networks (a long main feeder and a certain number of short laterals) two measurement units, located at the beginning and at the end of the main feeder, may be sufficient. Method A locates the lateral where the fault occurs whereas method B could be applied in order to estimate its location on the identified lateral.

For the specific case of Figure 3, and for the case of a three-phase short circuit in L3, by using only units S_S and S_5, method A identifies a fault 2003 m away from S_S. This position corresponds to the point where lateral L3 starts (2000 m away from S_S). The information obtained by using method A suggests also which, of the distance values identified by method B (applied to the transient recorded at S_S), should be considered for this case, i.e. 2450.8 m. The fault location is then estimated about 450 m far from the beginning of L3.

This hybrid approach would result in a fault location system less expensive than method A and more efficient than method B.

REFERENCES

1. Sachdev M.S., Agarwal R.: *A technique for estimating transmission line fault locations from digital impedance relay measurements.* IEEE Trans. on Power Delivery, vol. 3, n. 1, pp. 121–129, January 1988.
2. Srinivasan K., St.-Jacques A.: *A new fault location algorithm for radial transmission lines with loads.* IEEE Trans. on Power Delivery, vol. 4, n. 3, pp. 1676–1682, July 1989.
3. Girgis A.A., Hart D.G., Peterson W.L.: *A new fault location technique for two- and three-terminal lines.* IEEE Trans. on Power Delivery, vol. 7, n. 1, pp. 98–107, January 1992.
4. Ancell G.B., Pahalawatha N.C.: *Maximum likelihood estimation of fault location on transmission lines using travelling waves.* IEEE Trans. on Power Delivery, vol. 9, n. 2, pp. 680–689, April 1994.
5. Chaari O., Meunier M., Brouaye F.: *Wavelets: a new tool for the resonant grounded power distribution systems relaying.* IEEE Trans. on Power Delivery, vol. 11–3, pp. 1301–1308, July 1996.
6. F. H. Magnago, A. Abur.: *Fault location using wavelets.* IEEE Trans. on Power Delivery, vol. 13, n. 4, pp. 1475–1480, October 1998.
7. Thomas D.W.P., Batty R.E., Christopoulos C., Wang A.: *A novel transmission-line voltage measuring method.* IEEE Trans. on Instrumentation and Measurement, vol. 47, n. 5, pp. 1265–1270, October 1998.
8. Ebron S., Lubkeman D.L., White M.: *A neural network approach to the detection of incipient faults on power distribution feeders.* IEEE Trans. on Power Delivery, vol. 5, n. 2, pp. 905–914, April 1990.
9. Chen Z., Maun J.-C.: *Artificial neural network approach to single-ended fault locator for transmission lines.* IEEE Trans. on Power Systems, vol. 15, n. 1, pp. 370–375, February 2000.
10. Kandil N., Sood V.K., Khorasani K., Patel R.V.: *Fault identification in an AC-DC transmission system using neural networks.* IEEE Trans. on Power Systems, vol.7, n. 2, pp. 812–819, May 2002.
11. Peretto L., Sasdelli R., Scala E., Tinarelli R.: *A distributed measurement system for locating transient-voltage sources.* Proc. of the 23rd IEEE IMTC/06, April 2006, Sorrento (Italy), pp. 1233–1238.
12. Borghetti A., Corsi S., Nucci C.A., Paolone M., Peretto L., Tinarelli R.: *On the use of continuous-wavelet transform for fault location in distribution power networks.* Proc. of the 15th Power System Computation

Conference — PSCC 2005, Liege, Belgium. Selected for publication on the Int. Journal on Electrical Power and Energy Systems, 2006.

13. Peretto L., Rinaldi P., Sasdelli R., Tinarelli R.: *A System for the Measurement of the Starting Instant of Impulsive Transients.* Proc. of the 21st IEEE IMTC/04, May 2004, Como (Italy), vol 2, pp. 1394–1398.
14. Angrisani L., Daponte P., D'Apuzzo M.: *Wavelet network-based detection and classification of transients.* IEEE Trans. on Instrumentation and Measurement, vol. 50, n. 5, October 2001, pp. 1425–1435.
15. Goupillaud P., Grossmann A., Morlet J.: *Cycle-octave and related transforms in seismic signal analysis.* Geoexploration, 23, 85–102, 1984–1985.
16. Daubechies I.: *The wavelet transform, time-frequency localization and signal analysis.* IEEE Trans. on Inf. Theory, vol.36, No.9, pp.961–1005, Sept. 1990.
17. Daubechies I.: *Orthonormal bases of compactly supported wavelets.* Comm. on Pure and Applied Math., vol.XLI, pp.909–996, 1988.
18. Clarke E.: *Circuit Analysis of A-C Power Systems*. Vol. 1. New York: John Wiley & Sons, 1943.
19. Mahseredjian J., Lefebvre S. and Do X.D.: *A new method for time-domain modeling of nonlinear circuits in large linear networks.* Proc of the 11th Power Systems Computation conference (PSCC), August 1993, Vol. 2, pp. 915–922.
20. Mahseredjian J., Dubé L., Gérin-Lajoie L.: *New advances in the Simulation of Transients with EMTP: Computation and Visualization Techniques*. Electrimacs, 19 August 2002.

Alberto Borghetti
was born in Cesena, Italy, in 1967. He graduated (with honours) in Electrical Engineering from the University of Bologna, Italy, in 1992. Since then he has been working with the power system group at the same University, where he was appointed Researcher in 1994 and Associate Professor of Electric Power Systems in 2004. Elected Senior member of IEEE in 2003, he is member of the IEEE PES WG on Distributed Resources: Modeling and Analysis, of the IEEE WG on Lightning performance of distribution lines, of the joint CIGRE-CIRED Working Group "Protection of MV and LV networks against Lightning", of the CIGRE WG C4.6.01 on Power System Security Assessment and he is Italian representative to the European COST Action P18 "The Physics of Lightning Flash and its Effects". His main research interests concern power system analysis, with particular reference to voltage collapse, power system restoration, electromagnetic transients and optimal generation scheduling.

Address:
Dept. of Electrical Engineerig, University of Bologna
viale Risorgimento, 2, 40136, Bologna, Italy
tel.: +39 051 209 3475, fax: +39 051 209 3470
e-mail: alberto.borghetti@unibo.it

Mauro Bosetti
was born in Trento, Italy, in 1978. Received the degree with honours in Electrical Engineering at the University of Bologna, Italy, in 2005. He is currently PhD student within the power system group in the same University. His research interests are distributed generation, with particular reference to micro-grid operation, and fault location.

Address:
Dept. of Electrical Engineerig, University of Bologna
viale Risorgimento, 2, 40136, Bologna, Italy
tel.: +39 051 209 3738, fax: +39 051 209 3470
e-mail: mauro.bosetti@mail.ing.unibo.it

Mauro Di Silvestro
was born in Giulianova, Italy, in 1980. Received a degree with honours in Electrical Engineering at the University of Bologna in 2005. He is currently working within the power systems group of the University of Bologna. His research interests are power system transients, with particular reference to fault location and distributed generation.

Address:
Dept. of Electrical Engineerig, University of Bologna
viale Risorgimento, 2, 40136, Bologna, Italy
tel.: +39 051 209 3738, fax: +39 051 209 3470
e-mail: mauro.disilvestro@guest.ing.unibo.it

Carlo Alberto Nucci
was born in Bologna, Italy, in 1956. Degree with honours in Electrical engineering in 1982 from the University of Bologna. Researcher in the Power Electrical Engineering Institute in 1983. Associate professor in the same University in 1992, full professor, chair of Power Systems, in 2000. He is author or co-author of more than 200 scientific papers published on reviewed journals or presented at international conferences. He is member of the IEEE Working Group 'Lightning performance of Distribution lines' and of the CIGRE Working group C.401 'Lightning' (of which he is also convener). His research interests concern power systems transients and dynamics, with particular reference to lightning impact on power lines, system restoration after black-out and distributed generation. He is the chair of International Steering Committee of the IEEE PowerTech and of the IEEE PES Italian Chapter PE31 in Region 8. He was the recipient of the 2004 IEEE CIGRE Technical Committee Award. Since January 2005 he is regional editor for Africa and Europe of the Electric Power System Research journal, Elsevier.

Address:
Dept. of Electrical Engineerig, University of Bologna
viale Risorgimento, 2, 40136, Bologna, Italy
tel.: +39 051 209 3479, fax: +39 051 209 3470
e-mail: carloalberto.nucci@unibo.it

Mario Paolone
was born in Campobasso, Italy, in 1973. Received a degree with honours in electrical engineering in 1998, and the PhD degree from the same University in 2002. He is currently working within the power systems group of the University of Bologna. He is member of the IEEE WG on Lightning performance of distribution lines and of the joint CIGRE-CIRED Working Group "Protection of MV and LV networks against Lightning". His research interests are power system transients, with particular reference to LEMP-interaction with electrical networks, power systems dynamics, power system protections and distributed generation.

Address:
Dept. of Electrical Engineerig, University of Bologna
viale Risorgimento, 2, 40136, Bologna, Italy
tel.: +39 051 209 3477, fax: +39 051 209 3470
e-mail: mario.paolone@unibo.it

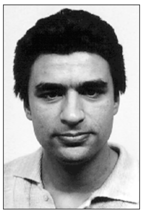

Lorenzo Peretto (M'98) (SM'03)
received the laurea degree in electronic engineering and the Ph.D. degree in electrical engineering from the University of Bologna, Italy, in 1993 and 1997, respectively. In 1998 he joined the Department of Electrical Engineering of the University of Bologna as an Assistant Professor with the Electrical and Electronic Measurement Group and since January 2004 as an Associate Professor. His fields of research are digital signal processing, measurements for the analysis of Power Quality, distributed measurement instrumentation; design of new electromagnetic-fields sensors and instrumentation; reliability prediction electronic systems;

Address:
Department of Electrical Engineering, University of Bologna,
Viale Risorgimento 2, Bologna, Italy.
e-mail: lorenzo.pereto@mail.ing.unibo.it
tel.: +39 051 20 93483, fax: +39 051 20 93588

Elisa Scala
was born in Bologna, Italy, in 1979. In 2004 she received the MS degree in electrical engineering from the University of Bologna, where she is presently working in the Electric Engineering Department as Ph.D. Student. Her main research topics are: design, development and novel metrological characterization techniques of instrumentation for measurement under non-sinusoidal conditions; digital signal processing and measurements for the analysis of Power Quality; distributed measurement instrumentation; design of new electric-field sensors and instrumentation.

Address:
Dept. of Electrical Engineering, University of Bologna
viale Risorgimento, 2, 40136, Bologna, Italy
tel.: +39 051 209 3472, fax: +39 051 209 3470
e-mail: elisa.scala@mail.ing.unibo.it

Roberto Tinarelli (S'02, M'05)
was born in Bologna, Italy, in 1974. He received the MS degree and the Ph.D. degree in electrical engineering from the University of Bologna and the Polytechnic of Milan, Italy, respectively, in 2000 e 2004, respectively.

He is author or co-author of more than 50 scientific papers, many of them presented at international conferences or published on reviewed journals. In 2000, he joined the Dipartimento di Ingegneria Elettrica of the University of Bologna where he is presently a Contract Researcher.

His research activity is mainly devoted to: design and metrological characterization of instruments for measurement under nonsinusoidal conditions; design and development of new instrumentation for flicker measurement. Dr. Tinarelli is a member of GMEE, the Italian association of Electrical and Electronic Measurement.

Address:
Dept. of Electrical Engineering, University of Bologna
viale Risorgimento, 2, 40136, Bologna, Italy
tel.: +39 051 209 3488, fax: +39 051 209 3470
e-mail: Roberto.tinarelli@mail.ing.unibo.it